

Article

Crystal Structure and Theoretical Analysis of $\text{Cs}_2\text{Ca}_3(\text{SO}_4)_4$

Penglin Fang [†], Wenyue Tang [†], Yaoguo Shen ^{* }, Jinquan Hong ^{*}, Yongming Li and Junrong Jia ^{*}

College of Physics and Electronic Information Engineering, Minjiang University, Fuzhou 350108, China; 3262193848@qq.com (P.F.); 2824749908@qq.com (W.T.); 1544971187@qq.com (Y.L.)

* Correspondence: shenyg@mju.edu.cn (Y.S.); jqhong@mju.edu.cn (J.H.); jiajr@mju.edu.cn (J.J.)

[†] These authors contributed equally.

Abstract: Using the homovalent cation substitution strategy, a new sulfate, $\text{Cs}_2\text{Ca}_3(\text{SO}_4)_4$, was successfully prepared using the spontaneous crystallization technique. A single-crystal structure measurement suggested that it crystallizes in space group $P2_1/c$, with lattice parameters and molecules per unit cell of $a = 9.9153(8)$, $b = 9.3760(6)$, $c = 9.8044(9)$, $\beta = 118.365(3)^\circ$, $V = 802.04(11)$, and $Z = 2$. In the structure of $\text{Cs}_2\text{Ca}_3(\text{SO}_4)_4$, CaO_6 octahedra and SO_4 tetrahedra are interconnected via a corner-sharing mode to form a three-dimensional framework comprising large cavities filled with Cs^+ cations. First-principles calculations and diffuse reflectance spectra indicated that $\text{Cs}_2\text{Ca}_3(\text{SO}_4)_4$ has a large energy band gap. Moreover, structural comparisons with similar compounds were conducted to explain the role of cations in tuning structural symmetry and birefringence. This paper helps to explain the size effect of cations on structural evolution.

Keywords: crystal structure; structure-property relationship; sulfate; energy band; birefringence



Citation: Fang, P.; Tang, W.; Shen, Y.; Hong, J.; Li, Y.; Jia, J. Crystal Structure and Theoretical Analysis of $\text{Cs}_2\text{Ca}_3(\text{SO}_4)_4$. *Crystals* **2022**, *12*, 126. <https://doi.org/10.3390/cryst12020126>

Academic Editors: Shujun Zhang and Andrei Vladimirovich Shevelkov

Received: 10 December 2021

Accepted: 16 January 2022

Published: 18 January 2022

Publisher's Note: MDPI stays neutral with regard to jurisdictional claims in published maps and institutional affiliations.



Copyright: © 2022 by the authors. Licensee MDPI, Basel, Switzerland. This article is an open access article distributed under the terms and conditions of the Creative Commons Attribution (CC BY) license (<https://creativecommons.org/licenses/by/4.0/>).

1. Introduction

Sulfates have been used for a wide range of purposes since ancient times. For example, potassium sulfate can be used as a chemical fertilizer for plants, promoting plant growth and crop yield. More recently, sulfates have been considered suitable for use as ultraviolet birefringent materials based on certain merits, including that they are environmentally friendly raw chemical materials, have a wide transparency window, and easily grow as crystals. A series of excellent birefringent materials have been reported so far, including $\text{NH}_4\text{NaLi}_2(\text{SO}_4)_2$ [1], ASbF_2SO_4 ($A = \text{Rb}, \text{Cs}$) [2,3], $\text{K}_2\text{Bi}_2(\text{SO}_4)_2\text{Cl}_4$ [4], $\text{Nb}_2\text{O}_3(\text{IO}_3)_2(\text{SO}_4)$ [5], and $\text{Ce}(\text{SO}_4)\text{F}_2$ [6]. Aside from changing the cation type, introducing organic π -conjugated units into sulfates is also an effective way to produce new materials possessing high birefringence. For example, using a combination of inorganic sulfates and neutral thiourea molecules, a birefringence of 0.21 at 546.1 nm in $\text{Te}(\text{CS}(\text{NH}_2)_2)_4\text{SO}_4 \cdot 2\text{H}_2\text{O}$ [7] and 0.16 at 554 nm in $\text{Zn}[\text{CS}(\text{NH}_2)_2]_3\text{SO}_4$ can be achieved [8]. However, most of these sulfates have relatively long UV absorption edges, which is not conducive to application in the UV region. Therefore, the search for short-wave UV sulfates is still ongoing.

Since the SO_4 groups in sulfates exist only as monomers, cations play an important role in the synthesis of new compounds. In order to obtain sulfates with short UV absorption edges, the choice of counterpart cation is best confined to those metal elements in the first or second main group [9–11]. Numerous experiments have confirmed that metal cations without $d-d$ or $f-f$ electron transitions barely damage the UV absorption edge of the $[\text{SO}_4]^{2-}$ anionic group [12–14]. Based on the abovementioned idea, sulfates of single/mixed alkali metals were synthesized using the slow aqueous evaporation technique. Moreover, NH_4^+ cations were introduced into the sulfates to tune the structure and the optical properties [1,4,15–17]. Pure alkali metal sulfates exhibit low thermal stability, which can be elevated by introducing alkali earth metal elements into the sulfates [14,18,19]. Because alkali earth sulfates have low solubility in water, they are often prepared using a

traditional high-temperature molten method, such as $A_2M_2(SO_4)_3$ ($A = Rb, Cs$; $M = Mg, Ca$) and $Cs_2Mg_3(SO_4)_4$ [14,18–20].

According to the cation substitution strategy, in which cations in the same family have a similar coordination environment, we intended to synthesize a new compound, $Cs_2Ca_3(SO_4)_4$, by substituting Ca^{2+} for Mg^{2+} cations in $Cs_2Mg_3(SO_4)_4$ [18]. By changing the ratio of raw materials, $Cs_2Ca_3(SO_4)_4$ crystals were successfully prepared using the spontaneous crystallization technique. First-principles calculations demonstrated that $Cs_2Ca_3(SO_4)_4$ showed a greatly enhanced birefringence compared to $Cs_2Mg_3(SO_4)_4$, which was analyzed using detailed structural comparisons. Both the UV–vis–NIR diffuse reflectance spectrum and electronic band structure verified that $Cs_2Ca_3(SO_4)_4$ has a large energy band gap. This work may serve as a useful reference for understanding the role of cations in regulating crystal structures and optical properties.

2. Materials and Methods

Single crystals of $Cs_2Ca_3(SO_4)_4$ were grown in an open environment using the spontaneous crystallization technique. First, the raw materials of Cs_2SO_4 and $CaSO_4$ at a molar ratio of 1:3 were finely ground and then left at 973 K for 3 days to obtain the nominal $Cs_2Ca_3(SO_4)_4$ polycrystalline product. Second, $Cs_2Ca_3(SO_4)_4$ powder was mixed with Cs_2SO_4 and then melted in a program-controlled muffle furnace at 1273 K for 2 days. Finally, $Cs_2Ca_3(SO_4)_4$ single crystals with a maximum size of 0.5 mm × 0.7 mm × 0.3 mm were obtained by slowly cooling the muffle furnace. The purity of the obtained crystals was checked by powder X-ray diffraction (XRD) data collected on a Rigaku MiniFlex II diffractometer (Cu $K\alpha$ radiation). A small crystal with dimensions of 0.08 mm × 0.06 mm × 0.06 mm was selected for single-crystal structure measurements, which were performed on a Bruker D8 with graphite-monochromatized Mo $K\alpha$ radiation ($\lambda = 0.71073 \text{ \AA}$). The structure was solved using SHELXS and SHELXL [21], and further checked using the PLATON program [22]. Detailed crystallographic information is given in Supplementary Tables S1–S4. CCDC 2126379 contains the supplementary crystallographic data for this paper. These data can be obtained free of charge at <http://www.ccdc.cam.ac.uk/conts/retrieving.html>, accessed on 14 December 2021, (or from the CCDC, 12 Union Road, Cambridge CB2 1EZ, UK; Fax: +44 1223 336033; e-mail: deposit@ccdc.cam.ac.uk). The UV–vis–NIR diffuse reflectance spectrum was measured on a PerkinElmer Lambda-950 spectrophotometer. The first-principles calculations were performed using the CASTEP suite in Material Studio [23,24]. The Perdew–Burke–Ernzerhof functional and generalized gradient approximation [25,26] was selected [27]. The kinetic energy absorption, k-point sampling, and pseudopotential used for calculating the electronic band structure and density of states were 300 eV, $1 \times 1 \times 1$, and ultrasoft, respectively. Detailed birefringence calculation settings can be found in the Supplementary Materials.

3. Results and Discussion

3.1. Powder XRD

Figure 1 shows the XRD patterns of the synthesized $Cs_2Ca_3(SO_4)_4$ crystals. The black pattern represents the experimental powder XRD, and the red pattern represents the XRD calculated from the single-crystal structure. The experimental XRD pattern basically reflects that of our obtained compound, but with additional minor miscellaneous peaks (marked with asterisks in Figure 1), which led us to compare the XRD patterns of the raw reagents (Cs_2SO_4 and $CaSO_4$) with the title compound. As shown in Supplementary Figure S1, the pattern of $Cs_2Ca_3(SO_4)_4$ is distinct from the patterns of the raw reagents, indicating that the additional peaks are caused by other compounds. Considering our previously reported compound, $Cs_2Ca_2(SO_4)_3$, was prepared using the same raw reagents, it is imperative that its characteristic peaks are properly distinguished from those corresponding to $Cs_2Ca_3(SO_4)_4$, newly synthesized here. In conclusion, the impurity peaks indicated in Figure 1 could be caused by $Cs_2Ca_2(SO_4)_3$ [14].

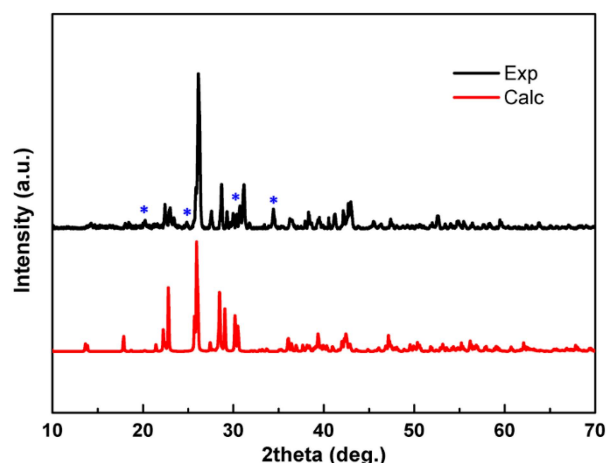


Figure 1. Calculated and experimental XRD patterns for $\text{Cs}_2\text{Ca}_3(\text{SO}_4)_4$.

3.2. Crystal Structure

Crystal data for $\text{Cs}_2\text{Ca}_3(\text{SO}_4)_4$ ($M = 770.30$ g/mol) are as follows: monoclinic, space group $P2_1/c$ (no. 14), $a = 9.9153(8)$ Å, $b = 9.3760(6)$ Å, $c = 9.8044(9)$ Å, $\beta = 118.365(3)^\circ$, $V = 802.04(11)$ Å³, $Z = 2$, $T = 299(2)$ K, $\mu(\text{MoK}\alpha) = 6.104$ mm⁻¹, $D_{\text{calc}} = 3.190$ g/cm³, 9439 reflections measured ($2.33^\circ \leq 2\theta \leq 27.45^\circ$), 1635 of them unique ($R_{\text{int}} = 0.0506$, $R_{\text{sigma}} = 0.0359$), which were used in all calculations. The final R_1 was 0.0438 ($I > 2\sigma(I)$) and wR_2 was 0.0864 (all data). The fundamental building units of $\text{Cs}_2\text{Ca}_3(\text{SO}_4)_4$ were CaO_6 octahedra and SO_4 tetrahedra. These groups are interconnected by sharing vertex oxygen atoms to form a three-dimensional framework with large cavities filled by Cs^+ cations (Figure 2). Each Cs^+ cation is coordinated to eight oxygen atoms to form a CsO_8 polyhedron, with Cs–O bond distances ranging from 3.026(5) to 3.354(5) Å (Supplementary Figure S2), because the next closest atom is not oxygen but sulfur, with a Cs–S bond distance of 3.6568(15) Å. The S–O bond lengths are in the range of 1.453(5)–1.478(5) Å and O–S–O bond angles vary from 105.4(4) to 112.3(3)°. Each Ca atom is bound to six O atoms to generate a CaO_6 octahedron, with Ca–O bond lengths ranging from 2.276(5) to 2.526(5) Å. These bond distances and angles appear reasonable when compared with those reported for other sulfates [14,18,20].

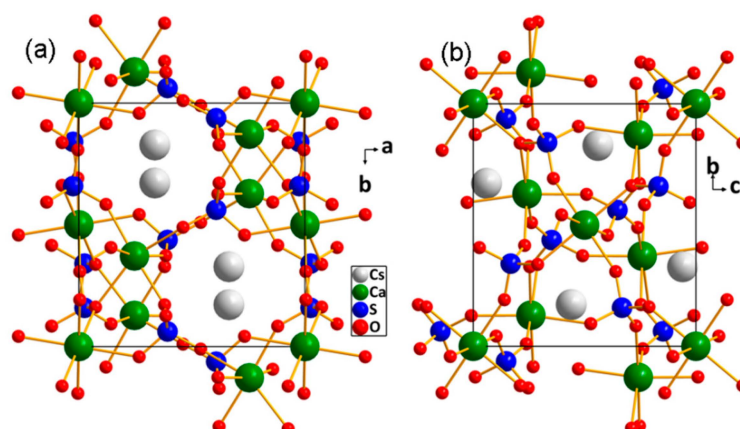


Figure 2. Crystal structure of $\text{Cs}_2\text{Ca}_3(\text{SO}_4)_4$ viewed along (a) c -axis and (b) a -axis.

After comparing the structures of $\text{Cs}_2\text{Mg}_3(\text{SO}_4)_4$, $\text{Cs}_2\text{Ca}_3(\text{SO}_4)_4$, and $\text{Rb}_2\text{Mg}_3(\text{SO}_4)_4$, some interesting things were discovered [18]. First, $\text{Cs}_2\text{Mg}_3(\text{SO}_4)_4$ and $\text{Cs}_2\text{Ca}_3(\text{SO}_4)_4$ have distinct lattice types. The structure of the former belongs to a non-centrosymmetric $P2_12_12_1$ space group, while the latter crystallizes in a centrosymmetric $P2_1/c$ space group. Although they have similar three-dimensional frameworks made up of alkaline earth metal cation-

centered polyhedra and SO_4 tetrahedra, the connection mode is quite different. Figure 3 shows a structural comparison with regard to the coordination environment of alkali earth metal cations (Mg^{2+} vs. Ca^{2+}). In $\text{Cs}_2\text{Mg}_3(\text{SO}_4)_4$, each Mg^{2+} cation is 4/5-fold coordinated to form MgO_5 or MgO_6 polyhedron, which is connected to five SO_4 groups (Figure 3c,d). Interestingly, corner-sharing mode is used when the Mg_2O_6 octahedra link with four SO_4 groups, and the linking with the additional SO_4 group (five altogether) occurs through edge-sharing mode. In addition, the Mg1 atom connects to one Mg2 atom via a common oxygen atom (Figure 3d). When Mg^{2+} cations are replaced by Ca^{2+} cations of large radii in constructing the new compound $\text{Cs}_2\text{Ca}_3(\text{SO}_4)_4$, CaO_6 octahedra connect to adjacent SO_4 groups exclusively by corner-sharing mode because of the extended Ca–O bond distances. Moreover, the Ca2 atom in $\text{Cs}_2\text{Ca}_3(\text{SO}_4)_4$ bridges two adjacent Ca atoms, which is not observed in $\text{Cs}_2\text{Mg}_3(\text{SO}_4)_4$. The longer Ca–O bond makes the SO_4 groups arrange more uniformly than those in $\text{Cs}_2\text{Mg}_3(\text{SO}_4)_4$. Second, $\text{Cs}_2\text{Ca}_3(\text{SO}_4)_4$ is isomorphous to $\text{Rb}_2\text{Mg}_3(\text{SO}_4)_4$, in which MO_6 ($\text{M} = \text{Ca}, \text{Mg}$) octahedra connect to adjacent SO_4 tetrahedra via corner-sharing mode (Figure 3e,f). The only difference is that MO_6 octahedra have a different distortion, resulting from uneven bond distances. In $\text{Rb}_2\text{Mg}_3(\text{SO}_4)_4$, one Mg1–O bond distance (2.510 Å) is apparently longer than the other Mg–O bonds, which induces a large distortion of Mg_1O_6 octahedra. Such distortion is beneficial to the polarization anisotropy. In addition, the cation radius ratio of Cs/Ca, Rb/Mg, and Cs/Mg is 1.707, 2.27, and 2.60, respectively, indicating that the larger the difference in cation radius, the more easily the non-centrosymmetric structure is formed.

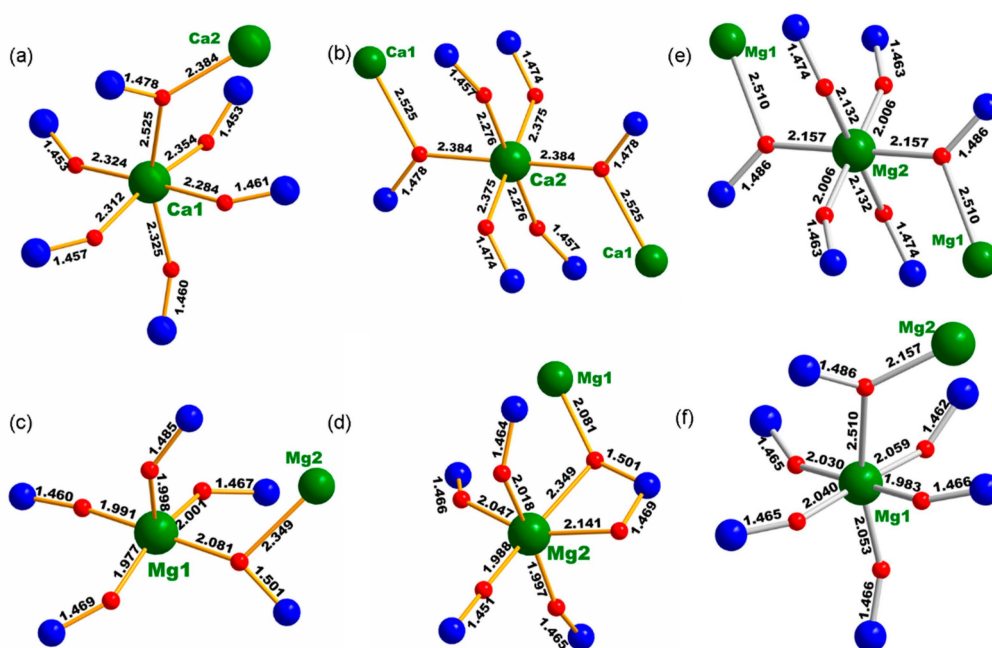


Figure 3. Connection mode between (a,b) Ca and S atoms in $\text{Cs}_2\text{Ca}_3(\text{SO}_4)_4$ and between Mg and S atoms in (c,d) $\text{Cs}_2\text{Mg}_3(\text{SO}_4)_4$ and (e,f) $\text{Rb}_2\text{Mg}_3(\text{SO}_4)_4$.

3.3. UV–vis–NIR Diffuse Reflectance Spectroscopy

When light is projected onto a rough surface, it is reflected in all directions, which is referred to as diffuse reflectance. The measured UV–vis–NIR diffuse reflectance spectrum is depicted in Figure 4. Apparently, the reflectance of $\text{Cs}_2\text{Ca}_3(\text{SO}_4)_4$ is close to 100% in the wavelength range of 400–800 nm and higher than 60% in the range of 200–400 nm. Although the synthesized samples had low levels of $\text{Cs}_2\text{Ca}_2(\text{SO}_4)_3$, this impurity exhibited a higher reflectance than our measured value and, thus, the measured spectrum essentially shows reflectance due to $\text{Cs}_2\text{Ca}_3(\text{SO}_4)_4$. Therefore, it can be inferred that the energy band

gap is greater than 6.2 eV, suggesting that $\text{Cs}_2\text{Ca}_3(\text{SO}_4)_4$ has a wide UV light window of penetration and may have a potential application as a window material.

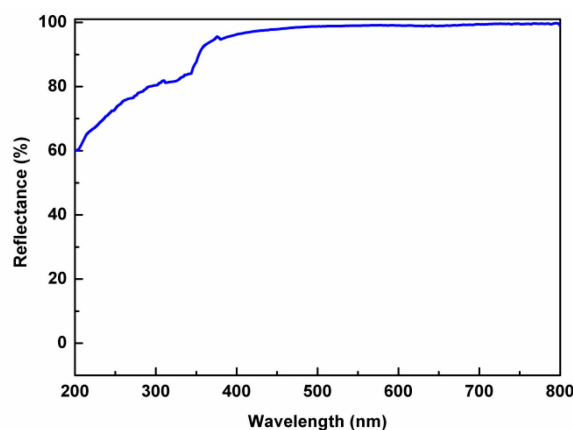


Figure 4. Diffuse reflectance spectrum of $\text{Cs}_2\text{Ca}_3(\text{SO}_4)_4$.

3.4. Electronic Structure

Electronic structures can be used to verify diffuse reflectance spectra and understand the origin of optical properties. The energy band structure calculation demonstrates that the title compound exhibits a large band gap of 5.453 eV. Although the calculated value is slightly smaller than the experimental one, it basically verifies that $\text{Cs}_2\text{Ca}_3(\text{SO}_4)_4$ has a high reflectance in the UV region (Figure 5a). The total density of states (DOS) and partial DOS are shown in Figure 5b. In the energy region from -20 to -15 eV, the contribution of Ca-3p, Cs-5s, S-2p, and O-1s states dominates (Figure 5b). In the energy region from -10 to -5 eV, the DOS is mainly composed of Cs-6p, S-2p, and O-2p states. In the energy range from -5 to 0 eV, only O-2p states contribute. In the energy range from 5 to 10 eV, Cs-6s and Cs-6p states take up most of the DOS, while the contribution from S, O, and Ca elements gradually decreases. As we know, the optical absorption edge is closely related to the energy band gap determined by the states around the Fermi level [28]. From the above analysis, in the range of -5 to 10 eV, the elements S, O, and Cs make the largest contribution and, thus, determine the energy band gap of the title compound. In other words, SO_4 groups and Cs^+ cations represent the main contribution in determining the optical properties of $\text{Cs}_2\text{Ca}_3(\text{SO}_4)_4$.

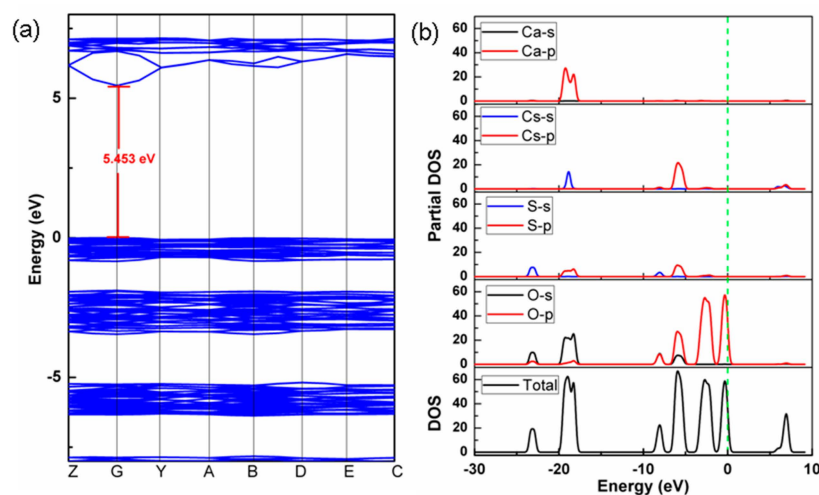


Figure 5. (a) Electronic band structure; (b) DOS and partial DOS plots.

The birefringence of $\text{Cs}_2\text{Ca}_3(\text{SO}_4)_4$ and two similar compounds was calculated. As shown in Figure 6, the birefringence of the three compounds increases with the decreased in-

cident wavelength, and the values are 0.0016 at 534 nm for $\text{Cs}_2\text{Mg}_3(\text{SO}_4)_4$, 0.0043 at 534 nm for $\text{Cs}_2\text{Ca}_3(\text{SO}_4)_4$, and 0.0175 at 534 nm for $\text{Rb}_2\text{Mg}_3(\text{SO}_4)_4$. Apparently, $\text{Cs}_2\text{Ca}_3(\text{SO}_4)_4$ has a birefringence higher than that of $\text{Cs}_2\text{Mg}_3(\text{SO}_4)_4$ but lower than that of $\text{Rb}_2\text{Mg}_3(\text{SO}_4)_4$, which results from the distinct anisotropy polarization of cationic polyhedra and the arrangement of SO_4 groups. It is well known that SO_4 groups in sulfates exist only as isolated units, so cations have a dominant role in controlling their arrangement.

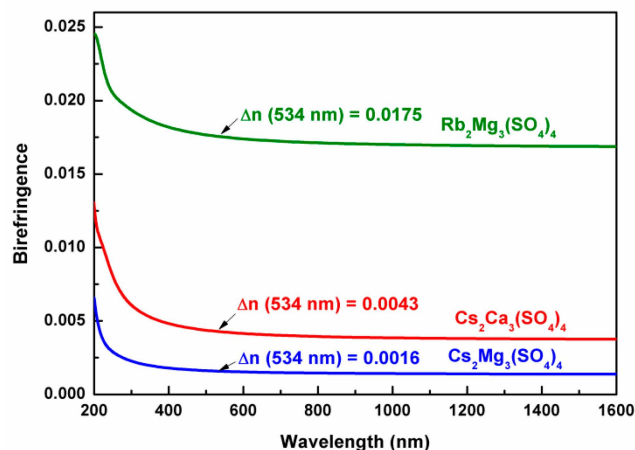


Figure 6. Calculated birefringence for $\text{Cs}_2\text{Ca}_3(\text{SO}_4)_4$, $\text{Cs}_2\text{Mg}_3(\text{SO}_4)_4$, and $\text{Rb}_2\text{Mg}_3(\text{SO}_4)_4$.

4. Conclusions

Using an element substitution strategy with a template compound of $\text{Cs}_2\text{Mg}_3(\text{SO}_4)_4$, $\text{Cs}_2\text{Ca}_3(\text{SO}_4)_4$ crystals were synthesized using the spontaneous crystallization technique. The crystal structure has fundamental building units of CaO_6 octahedra and SO_4 groups, which are connected to each other through a corner-sharing mode. Structural comparisons indicate that the SO_4 groups in $\text{Cs}_2\text{Ca}_3(\text{SO}_4)_4$ are more uniformly arranged than those in $\text{Cs}_2\text{Mg}_3(\text{SO}_4)_4$, which may be the reason for the sharply enhanced birefringence. The measured UV–vis–NIR diffuse reflectance spectrum shows that the title compound has a wide transparency window in the UV optical region. The first-principles calculations suggest that Cs^+ cations and SO_4 groups are responsible for the large energy band gap of $\text{Cs}_2\text{Ca}_3(\text{SO}_4)_4$. This work may provide a useful reference for understanding the role of cations in regulating crystal structures and optical properties.

Supplementary Materials: The following are available online at <https://www.mdpi.com/article/10.3390/cryst12020126/s1>. Figure S1: Comparison of XRD patterns with raw reagents of Cs_2SO_4 and CaSO_4 , Figure S2: Ball-and-stick representation of CsO_8 polyhedron in $\text{Cs}_2\text{Ca}_3(\text{SO}_4)_4$, Table S1: Crystal data and structure refinement for $\text{Cs}_2\text{Ca}_3(\text{SO}_4)_4$, Table S2: Atom coordinates and equivalent isotropic displacement parameters for $\text{Cs}_2\text{Ca}_3(\text{SO}_4)_4$, Table S3: Selected bond distances and angles for $\text{Cs}_2\text{Ca}_3(\text{SO}_4)_4$, Table S4: Anisotropic displacement parameters for $\text{Cs}_2\text{Ca}_3(\text{SO}_4)_4$.

Author Contributions: Writing—original draft preparation, P.F.; investigation, W.T.; writing—review and editing, Y.S.; conceptualization, J.H.; methodology, Y.S. and J.J.; software, Y.L.; supervision, Y.S.; funding acquisition, Y.S. and J.H.; P.F. and W.T. contributed equally to this manuscript. All authors have read and agreed to the published version of the manuscript.

Funding: This research was funded by the Research Start-up Funds for Introducing Talents, Minjiang University, Fujian Province, China, grant numbers MJY21029 and MJY19014; the Natural Science Foundation, Fujian Province, China, grant numbers 2021J011029 and 2019J01762; and the Middle-aged and Young Teachers' Project, Fujian Province, China, grant number JAT200407.

Institutional Review Board Statement: Not applicable.

Informed Consent Statement: Not applicable.

Data Availability Statement: Not applicable.

Acknowledgments: We acknowledge the support from theoretical calculations conducted by Sangen Zhao at the Fujian Institute of Material Structure.

Conflicts of Interest: The authors declare no conflict of interest.

References

1. Li, Y.; Liang, F.; Zhao, S.; Li, L.; Wu, Z.; Ding, Q.; Liu, S.; Lin, Z.; Hong, M.; Luo, J. Two non- π -conjugated deep-UV nonlinear optical sulfates. *J. Am. Chem. Soc.* **2019**, *141*, 3833–3837. [[CrossRef](#)]
2. Dong, X.; Huang, L.; Hu, C.; Zeng, H.; Lin, Z.; Wang, X.; Ok, K.M.; Zou, G. CsSbF₂SO₄: An excellent ultraviolet nonlinear optical sulfate with a KTiOPO₄ (KTP)-type structure. *Angew. Chem.* **2019**, *131*, 6598–6604. [[CrossRef](#)]
3. Yang, F.; Huang, L.; Zhao, X.; Huang, L.; Gao, D.; Bi, J.; Wang, X.; Zou, G. An energy band engineering design to enlarge the band gap of KTiOPO₄ (KTP)-type sulfates via aliovalent substitution. *J. Mater. Chem. C* **2019**, *7*, 8131–8138. [[CrossRef](#)]
4. Chen, K.C.; Yang, Y.; Peng, G.; Yang, S.D.; Yan, T.; Fan, H.X.; Lin, Z.S.; Ye, N. A₂Bi₂(SO₄)₂Cl₄ (A = NH₄, K, Rb): Achieving a subtle balance of the large second harmonic generation effect and sufficient birefringence in sulfate nonlinear optical materials. *J. Mater. Chem. C* **2019**, *7*, 9900–9907. [[CrossRef](#)]
5. Tang, H.X.; Zhang, Y.X.; Zhuo, C.; Fu, R.B.; Lin, H.; Ma, Z.J.; Wu, X.T. A niobium oxyiodate sulfate with a strong second-harmonic-generation response built by rational multi-component design. *Angew. Chem. Int. Ed.* **2019**, *58*, 3824–3828. [[CrossRef](#)]
6. Wu, C.; Wu, T.H.; Jiang, X.X.; Wang, Z.J.; Sha, H.Y.; Lin, L.; Lin, Z.S.; Huang, Z.P.; Long, X.F.; Humphrey, M.G.; et al. Large second-harmonic response and giant birefringence of CeF₂(SO₄) induced by highly polarizable polyhedra. *J. Am. Chem. Soc.* **2021**, *143*, 4138–4142. [[CrossRef](#)] [[PubMed](#)]
7. Weng, X.Y.; Lin, C.S.; Peng, G.; Fan, H.X.; Zhao, X.; Chen, K.C.; Luo, M.; Ye, N. Te(CS(NH₂)₂)₄SO₄·2H₂O: A three-in-one semiorganic nonlinear optical crystal with an unusual quadrilateral (TeS₄)⁶⁻ chromophore. *Cryst. Growth Des.* **2021**, *21*, 2596–2601. [[CrossRef](#)]
8. Ramajothi, J.; Dhanuskodi, S.; Nagarajan, K. Crystal growth, thermal, optical and microhardness studies of tris (thiourea) zinc sulphate—A semiorganic NLO material. *Cryst. Res. Technol.* **2004**, *39*, 414–420. [[CrossRef](#)]
9. Peng, G.; Lin, C.-S.; Yang, Y.; Zhao, D.; Lin, Z.; Ye, N.; Huang, J.-S. Y₂(CO₃)₃·H₂O and (NH₄)₂Ca₂Y₄(CO₃)₉·H₂O: Partial aliovalent cation substitution enabling evolution from centrosymmetry to noncentrosymmetry for nonlinear optical response. *Chem. Mater.* **2019**, *31*, 52–56. [[CrossRef](#)]
10. Lu, J.; Yue, J.-N.; Xiong, L.; Zhang, W.-K.; Chen, L.; Wu, L.-M. Uniform alignment of non- π -conjugated species enhances deep ultraviolet optical nonlinearity. *J. Am. Chem. Soc.* **2019**, *141*, 8093–8097. [[CrossRef](#)] [[PubMed](#)]
11. Zhang, M.; An, D.H.; Hu, C.; Chen, X.L.; Yang, Z.H.; Pan, S.L. Rational design via synergistic combination leads to an outstanding deep-ultraviolet birefringent Li₂Na₂B₂O₅ material with an unvalued B₂O₅ functional gene. *J. Am. Chem. Soc.* **2019**, *141*, 3258–3264. [[CrossRef](#)]
12. Yang, Y.C.; Liu, X.; Lu, J.; Wu, L.M.; Chen, L. [Ag(NH₃)₂]₂SO₄: A strategy for the coordination of cationic moieties to design nonlinear optical materials. *Angew. Chem. Int. Ed.* **2021**, *60*, 21216–21220. [[CrossRef](#)] [[PubMed](#)]
13. Li, Y.; Zhao, S.; Shan, P.; Li, X.; Ding, Q.; Liu, S.; Wu, Z.; Wang, S.; Li, L.; Luo, J. Li₈NaRb₃(SO₄)₆·2H₂O as a new sulfate deep-ultraviolet nonlinear optical material. *J. Mater. Chem. C* **2018**, *6*, 12240–12244. [[CrossRef](#)]
14. Shen, Y.G.; Xue, X.L.; Tu, W.Y.; Liu, Z.Q.; Yan, R.W.; Zhang, H.; Jia, J.R. Synthesis, crystal structure, and characterization of a noncentrosymmetric sulfate Cs₂Ca₂(SO₄)₃. *Eur. J. Inorg. Chem.* **2020**, *2020*, 854–858. [[CrossRef](#)]
15. Sudhakar, K.; Nandhini, S.; Muniyappan, S.; Arumanayagam, T.; Vivek, P.; Murugakoothan, P. Synthesis, crystal growth, optical, thermal, and mechanical properties of a nonlinear optical single crystal: Ammonium sulfate hydrogen sulphamate (ASHS). *Appl. Phys. A Mater.* **2018**, *124*, 334. [[CrossRef](#)]
16. He, F.F.; Wang, Q.; Hu, C.F.; He, W.; Luo, X.Y.; Huang, L.; Gao, D.J.; Bi, J.; Wang, X.; Zou, G.H. Centrosymmetric (NH₄)₂SbCl(SO₄)₂ and non-centrosymmetric NH₄SbCl₂SO₄: Synergistic effect of hydrogen-bonding interactions and lone-pair cations on the framework structures and macroscopic centricities. *Cryst. Growth Des.* **2018**, *18*, 6239–6247. [[CrossRef](#)]
17. He, F.F.; Wang, L.; Hu, C.F.; Zhou, J.; Li, Q.; Huang, L.; Gao, D.J.; Bi, J.; Wang, X.; Zou, G.H. Cation-tuned synthesis of the A₂SO₄·SbF₃ (A = Na⁺, NH₄⁺, K⁺, Rb⁺) family with nonlinear optical properties. *Dalton Trans.* **2018**, *47*, 17486–17492. [[CrossRef](#)]
18. Wang, M.; Wei, D.Q.; Liang, L.J.; Yan, X.; Lv, K.K. Centrosymmetric Rb₂Mg₃(SO₄)₄ and non-centrosymmetric Cs₂Mg₃(SO₄)₄ with a phase-matching nonlinear optical response. *Inorg. Chem. Commun.* **2019**, *107*, 107486. [[CrossRef](#)]
19. Shen, Y.G.; Xue, X.L.; Yan, R.W.; Lin, H. Synthesis, characterizations and theoretical analysis of a noncentrosymmetric sulfate. *Inorg. Chem. Commun.* **2020**, *116*, 107899. [[CrossRef](#)]
20. Zhong, X.Y.; Wu, E.Q.; Yang, S.D.; Wang, H.H.; Lin, X.X.; Shen, Y.G. Optical properties and thermal stability of a cubic sulfate Rb₂Ca₂(SO₄)₃. *Chin. J. Struct. Chem.* **2021**, *40*, 949–954.
21. Sheldrick, G.M. A short history of SHELX. *Acta Crystallogr. Sec. A Found. Crystallogr.* **2008**, *64*, 112–122. [[CrossRef](#)]
22. Spek, A.L. Single-crystal structure validation with the program PLATON. *J. Appl. Crystallogr.* **2003**, *36*, 7–13. [[CrossRef](#)]
23. Payne, M.C.; Teter, M.P.; Allan, D.C.; Arias, T.A.; Joannopoulos, J.D. Iterative minimization techniques for ab initio total-energy calculations: Molecular dynamics and conjugate gradients. *Rev. Mod. Phys.* **1992**, *64*, 1045–1097. [[CrossRef](#)]
24. Clark, S.J.; Segall, M.D.; Pickard, C.J.; Hasnip, P.J.; Probert, M.J.; Refson, K.; Payne, M.C. First principles methods using CASTEP. *Z. Kristallogr. Cryst. Mater.* **2005**, *220*, 567–570. [[CrossRef](#)]

25. Ceperley, D.M.; Alder, B.J. Ground-state of the electron-gas by a stochastic method. *Phys. Rev. Lett.* **1980**, *45*, 566–569. [[CrossRef](#)]
26. Perdew, J.P.; Zunger, A. Self-interaction correction to density-functional approximations for many-electron systems. *Phys. Rev. B* **1981**, *23*, 5048–5079. [[CrossRef](#)]
27. Rappe, A.M.; Rabe, K.M.; Kaxiras, E.; Joannopoulos, J.D. Optimized pseudopotentials. *Phys. Rev. B* **1990**, *41*, 1227–1230. [[CrossRef](#)]
28. Lee, M.H.; Yang, C.H.; Jan, J.H. Band-resolved analysis of nonlinear optical properties of crystalline and molecular materials. *Phys. Rev. B* **2004**, *70*, 235110. [[CrossRef](#)]